Generalized Receiver Employment in Ultra-Wideband Systems: Performance Analysis

VYACHESLAV TUZLUKOV
Department of Technical Maintenance of Aviation and Radio Electronic Equipment
Belarusian State Aviation Academy
77, Uborevicha Str., 220096 Minsk
BELARUS

Abstract: - In the present paper, a performance analysis of an ultra-wideband (UWB) system based on the generalized approach to signal processing in noise is discussed. The UWB system utilizes a new pulse design that made the performance analysis possible, since the new not only has a short duration to reduce collision, but is also spectrally compliant to the standards on UWB systems. We present the performance analysis of the UWB system constructed based on the generalized receiver processing different pulse shapes and with various numbers of users. New simulation results on multiuser performance of the impulse radio are also presented.

1 Introduction

Ultra-wideband (UWB) technology [1] has recently become a darling of the telecommunications industry. Although under exploration since the 1980s, UWB technology was mainly considered for radar applications. However, recent development in high-speed switching technology has made UWB much more attractive for low-cost consumer communication applications [2]. One well-known approach, known as the UWB impulse radio, communicates by transmitting pulses of very short duration over ultra-wide bandwidth [3]. Since UWB radio signals require extremely broad bandwidth for transmission and must share a frequency spectrum with other existing systems [4], the well-known adopted standards have, thus far, restricted UWB systems to frequencies 3.1 GHz, respectively [1].

The Gaussian monocycle pulse, commonly used in UWB impulse radio [3], [5]-[7], must be modified and filtered to meet the standard requirements. Pulse shapers can be designed to meet the standard constraint. However, careless designing can extend the pulse duration and, thereby, lower the data rate. Parks-McClellan filtering of the Gaussian pulse by [8] has been successfully utilized. Its pulse spectrum closely matches the mask, but some scaling is needed to keep spectral ripples below the mask. Alternatively, in [9], there was presented a new algorithm to meet this pulse-design challenge utilizing the prolate spheriodal wave function of Slepian and Pollak [10], [11]. Here, the performance analysis of the UWB systems based on the generalized receiver is presented that utilize the new pulse design.

Generally, our approach can be extended to different pulse selections.

The remainder of this paper is organized as follows. In Section 2, the UWB pulse-design algorithm is discussed. In Section 3, the main functioning principles of the generalized receiver constructed based on the generalized approach to signal processing in noise are discussed. In Section 4, the performance of the UWB multiuser systems based on the generalized receiver is evaluated for two modulation schemes, utilizing one of the pulses numerically generated by our pulse-design algorithm. Design issues concerning the bit error rate (*BER*), with respect to the modulation scheme and the multiuser parameters, are discussed. In Section 5, simulation results of the multiuser UWB systems based on the generalized receiver are provided, along with multipath effects. In Section 6 some conclusions are discussed.

2 UWB Pulse-Design Algorithm

In [9], a new pulse-design algorithm is presented by utilizing prolate spheriodal wave functions [10], [11]. The standard spectral mask requires new pulse to have short durations while limited within 3.1-10.6 GHz. Our proposed design has several advantages for UWB pulse design over previous methods [5], [11]. Firstly, the pulse spectrum is concentrated in the desired frequency band, while the pulse duration can be controlled for high data rates. Secondly, our algorithm yields multiple orthogonal pulses that can be used for multiple user access. Thirdly, it provides pulse-design flexibility to fit frequency masks with single or multiple pass bands.

The pulse design begins with a desired frequency mask $H(f)$ or its corresponding impulse response $h(t)$. Our goal is to design a pulse signal $s^m(t)$ that is time limited to the pulse duration T_m, while exhibiting minimal distortion as it passes through the mask filter with impulse response $h(t)$. The short pulse duration is necessary as its inverse defines the maximum data rate through the UWB system based on the generalized receiver. Minimum distortion requires that when the pulse $s^m(t)$ is sent through the filter $h(t)$, the output should be $\lambda s^m(t)$ with only an attenuation factor λ. The pulse $s^m(t)$ is time limited to T_m. The output of the mask filter $h(t)$ is the convolution of the pulse $s^m(t)$ with the filter impulse response $h(t)$ as shown below

$$\lambda s^m(t) = \int_{-0.5T_m}^{0.5T_m} s^m(\tau)h(t-\tau)d\tau \quad . \qquad (1)$$

The closed-form solution to (1) is known as the prolate spheriodal wave function [9], [10]. For each eigenfunction $s^m(t)$, its eigenvalue λ defines the percentage of its energy contained within the frequency mask $H(f)$. The greater the eigenvalue, the better the power spectrum fits. Thus, only eigenvectors corresponding to the larger eigenvalues should be taken as pulse design for UWB. On the other hand, as eigenfunctions of the Hermitian function are real and the eigenfunctions corresponding to distinct eigen-values are orthogonal [12], the orthogonal eigenfunctions may be useful as the signalling pulses of multiple co-channel users in UWB systems based on the generalized approach to signal processing in noise.

Using this design algorithm for a bandpass frequency mask that coincides with standard regulations, we can design pulses [9] that have most of their power concentrated in the 3.1-10.6 GHz frequency band. To show the flexibility of our proposed algorithm, numerical examples are provided for a double pass band frequency mask. This frequency mask is represented in the frequency domain as follows:

$$H(f) = \begin{cases} 1, & 1\,GHz < f < 4\,GHz \\ 1, & 6\,GHz < f < 9\,GHz \\ 0, & elsewhere \end{cases} \qquad (2)$$

whose impulse response is also easily obtained.

Eigenvalue decomposition generates multiple eigenvectors whose spectra fit the desired frequency mask. We chose $T_m = 2$ nsec to achieve a good fit

with the desired frequency mask and plotted one of the suitable eigenvector pulses in Fig. 1. The corresponding power spectrum, Fig. 2, shows that the power spectral density is contained under the mask. This flexibility to design pulses that meet multiple pass bands distinguishes our algorithm from existing frequency-shift methods.
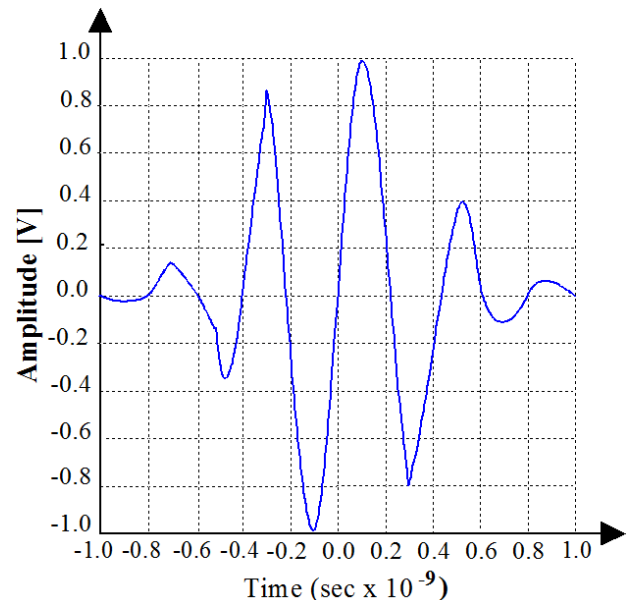
Fig. 1. Pulse shape obtained from the pulse-design algorithm using a double-passband frequency mask.
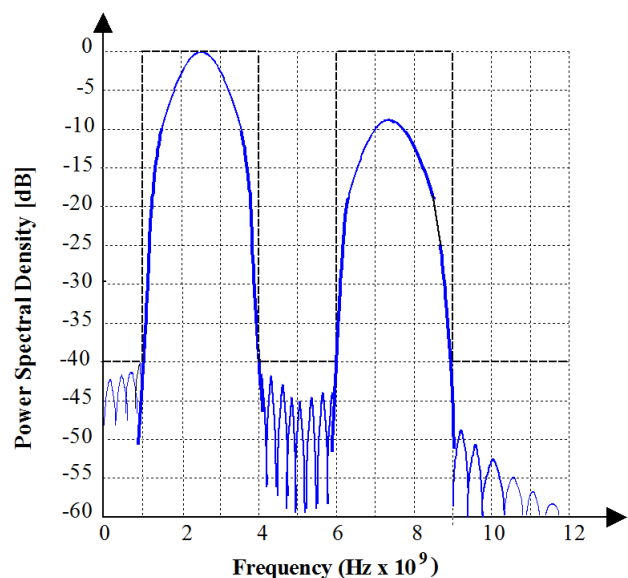
Fig. 2. Power spectral density of the pulse shape obtained from the pulse-design algorithm using a double-passband frequency mask.

3 Generalized Receiver: Main Functioning Principles

The generalized receiver is constructed in accordance with the generalized approach to signal processing in noise [13]-[15]. The generalized approach to signal processing in noise introduces an additional noise source that does not carry any information about the parameters of desired transmitted signal with the purpose to improve the signal processing system performance. This additional noise can be considered as the reference noise without any information about the parameters of the signal to be detected.

The jointly sufficient statistics of the mean and variance of the likelihood function is obtained under the generalized approach to signal processing in noise employment, while the classical and modern signal processing theories can deliver only the sufficient statistics of the mean or variance of the likelihood function. Thus, the generalized approach to signal processing in noise implementation allows us to obtain more information about the parameters of the desired transmitted signal incoming at the generalized receiver input. Owing to this fact, the detectors constructed based on the generalized approach to signal processing in noise technology are able to improve the signal detection performance of signal processing systems in comparison with employment of other conventional detectors.

The generalized receiver (GR) consists of three channels (see Fig. 3): the GR correlation detector channel (GR CD) – the preliminary filter (PF), the multipliers 1 and 2, the model signal generator (MSG); the GR energy detector channel (GR ED) – the PF, the additional filter (AF), the multipliers 3 and 4, the summator 1; and the GR compensation channel (GR CC) – the summators 2 and 3, the accumulator 1. The threshold apparatus (THRA) device defines the GR threshold.

As we can see from Fig.3, there are two bandpass filters, i.e., the linear systems, at the GR input, namely, the PF and AF. We assume for simplicity that these two filters or linear systems have the same amplitude-frequency characteristics or impulse responses. The AF central frequency is detuned relative to the PF central frequency.

There is a need to note the PF bandwidth is matched with the transmitted signal bandwidth. If the detuning value between the PF and AF central frequencies is more than 4 or 5 times the transmitted signal bandwidth to be detected, i.e., $4 \div 5\Delta f_s$, where Δf_s is the transmitted signal bandwidth, we can believe that the processes at the PF and AF outputs are uncorrelated because the coefficient of correlation between them is negligible (not more than 0.05). This fact was confirmed experimentally in [16] and [17] independently. Thus, the transmitted signal plus noise can be appeared at the GR PF output and the noise only is appeared at the GR AF output. The stochastic processes at the GR AF and GR PF outputs present the input stochastic samples from two independent frequency-time regions. If the discrete-time noise $w_i[k]$ at the GR PF and GR AF inputs is Gaussian, the discrete-time noise $\zeta_i[k]$ at the GR PF output is Gaussian too, and the reference discrete-time noise $\eta_i[k]$ at the GR AF output is Gaussian owing to the fact that the GR PF and GR AF are the linear systems and we believe that these linear systems do not change the statistical parameters of the input process. Thus, the GR AF can be considered as a generator of the reference noise with a priori information a "no" transmitted signal (the reference noise sample) [14, Chapter 5]. The noise at the GR PF and GR AF outputs can be presented as

$$
\begin{cases}
\zeta_i[k] = \sum_{m=-\infty}^{\infty} g_{PF}[m]w_i[k-m] \; ; \\
\eta_i[k] = \sum_{m=-\infty}^{\infty} g_{AF}[m]w_i[k-m] \; ,
\end{cases}
\tag{3}
$$

where $g_{PF}[m]$ and $g_{AF}[m]$ are the impulse responses of the GR PF and GR AF, respectively, and $w_i[k-m]$ is the noise at the generalized receiver input. In a general, under practical implementation of any detector in wireless communication system with sensor array, the bandwidth of the spectrum to be sensed is defined. Thus, the GR AF bandwidth and central frequency can be assigned, too (this bandwidth cannot be used by the transmitted signal because it is out of its spectrum). The case when there are interfering signals within the GR AF bandwidth, the action of this interference on the GR detection performance, and the case of non-ideal condition when the noise at the GR PF and GR AF outputs is not the same by statistical parameters are discussed in [18] and [19].

Under the hypothesis $\mathcal{H}_1$ ("a yes" transmitted signal), the GR CD generates the signal component $s_i^m[k]s_i[k]$ caused by interaction between the model signal $s_i^m[k]$, forming at the MSG output, and the incoming signal $s_i[k]$, and the noise component $s_i^m[k] \times \zeta_i[k]$ caused by interaction between the model signal $s_i^m[k]$ and the noise $\zeta_i[k]$ at the PF output. GR ED generates the transmitted signal energy $s_i^2[k]$ and

the random component $s_i[k]\zeta_i[k]$ caused by interaction between the transmitted signal $s_i[k]$ and the noise $\zeta_i[k]$ at the PF output. The main purpose of the GR CC is to cancel completely in the statistical sense the GR CD noise component $s_i^m[k]\zeta_i[k]$ and the GR ED random component $s_i[k]\zeta_i[k]$ based on the same nature of the noise $\zeta_i[k]$. The relation between the transmitted signal to be detected $s_i[k]$ and the model signal $s_i^m[k]$ is defined as:

$$s_i^m[k] = \mu \, s_i[k] \quad , \tag{4}$$

where μ is the coefficient of proportionality.

The main functioning condition under the GR employment in any signal processing system including the communication one with radar sensors is the equality between the parameters of the model signal $s_i^m[k]$ and the incoming signal $s_i[k]$, for example, by amplitude. Under this condition it is possible to cancel completely in the statistical sense the noise component $s_i^m[k]\zeta_i[k]$ of the GR CD and the random component $s_i[k]\zeta_i[k]$ of the GR ED. Satisfying the GR main functioning condition given by (4), $s_i^m[k] = s_i[k]$, $\mu = 1$, we are able to detect the transmitted signal with the high probability of detection at the low *SNR* and define the transmitted signal parameters with the required high accuracy.

Practical realization of the condition (4) at $\mu \to 1$ requires increasing in the complexity of GR structure and, consequently, leads us to increasing in computation cost. For example, there is a need to employ the amplitude tracking system or to use the off-line data samples processing. Under the hypothesis $\mathcal{H}_0$ ("a no" transmitted signal), satisfying the main

GR functioning condition (4) at $\mu \to 1$ we obtain only the background noise $\eta_i^2[k] - \zeta_i^2[k]$ at the GR output.

Under practical implementation, the real structure of GR depends on specificity of signal processing systems and their applications, for example, the radar sensor systems, adaptive wireless communication systems, cognitive radio systems, satellite communication systems, mobile communication systems and so on. In the present paper, the GR circuitry (Fig.3) is demonstrated with the purpose to explain the main functioning principles. Because of this, the GR flowchart presented in the paper should be considered under this viewpoint. Satisfying the GR main functioning condition (4) at $\mu \to 1$, the ideal case, for the wireless communication systems with radar sensor applications we are able to detect the transmitted signal with very high probability of detection and define accurately its parameters.

In the present paper, we discuss the GR implementation in the broadband space-time spreading MC DS-CDMA wireless communication system. Since the presented GR test statistics is defined by the signal energy and noise power, the equality between the parameters of the model signal $s_i^m[k]$ and transmitted signal to be detected $s_i[k]$, in particular by amplitude, is required that leads us to high circuitry complexity in practice.

For example, there is a need to employ the amplitude tracking system or off-line data sample processing. Detailed discussion about the main GR functioning principles if there is no a priori information and there is an uncertainty about the parameters of transmitted signal, i.e., the transmitted signal parameters are random, can be found in [13], [14, Chapter 6, pp.611–621 and Chapter 7, pp. 631–695].
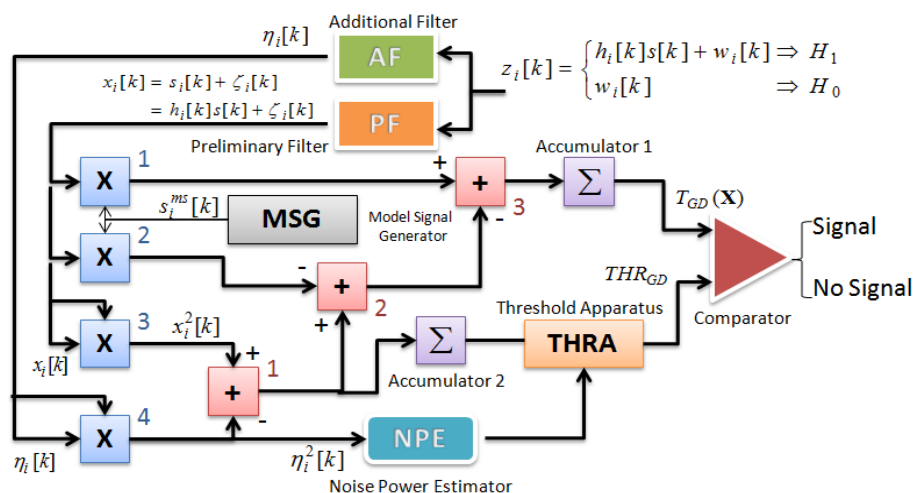
Fig. 3. Generalized receiver.

The complete matching between the model signal $s_i^m[k]$ and the incoming signal $s_i[k]$, for example by amplitude, is a very hard problem in practice because the incoming signal $s_i[k]$ depends on both the fading and the transmitted signal parameters and it is impractical to estimate the fading gain at the low *SNR*. This matching is possible in the ideal case only. The GD detection performance will be deteriorated under mismatching in parameters between the model signal $s_i^m[k]$ and the transmitted signal $s_i[k]$ and the impact of this problem is discussed in [20]-[23], where a complete analysis about the violation of the main GR functioning requirements is presented. The GR decision statistics requires an estimation of the noise variance σ_η^2 using the reference noise $\eta_i[k]$ at the AF output.

Under the hypothesis $\mathcal{H}_1$, the signal at the GR PF output, see Fig. 2, can be defined as

$$x_i[k] = s_i[k] + \zeta_i[k] \ , \qquad (5)$$

where $\zeta_i[k]$ is the noise at the PF output and

$$s_i[k] = h_i[k]s[k], \qquad (6)$$

where $h_i[k]$ are the channel coefficients. Under the hypothesis $\mathcal{H}_0$ and for all i and k, the process $x_i[k] = \zeta_i[k]$ at the PF output is subjected to the complex Gaussian distribution law and can be considered as the i.i.d. process.

In the ideal case, we can think that the signal at the GR AF output is the reference noise $\eta_i[k]$ with the same statistical parameters as the noise $\zeta_i[k]$. In practice, there is a difference between the statistical parameters of the noise $\eta_i[k]$ and $\zeta_i[k]$. How this difference impacts on the GR detection performance is discussed in detail in [14, Chapter 7, pp. 631 - 695] and in [20]-[26].

The decision statistics at the GR output presented in [16] and [17, Chapter 3] is extended for the case of antenna array when an adoption of multiple antennas and antenna arrays is effective to mitigate the negative attenuation and fading effects. The GR decision statistics can be presented in the following form:

$$T_{GR}(\mathbf{X}) = \sum_{k=0}^{N-1}\sum_{i=1}^{M} 2x_i[k]s_i^m[k]$$

$$-\sum_{k=0}^{N-1}\sum_{i=1}^{M}x_i^2[k] + \sum_{k=0}^{N-1}\sum_{i=1}^{M}\eta_i^2[k] \underset{\mathcal{H}_0}{\overset{\mathcal{H}_1}{\gtrless}} THR_{GR} \ , \qquad (7)$$

where

$$\mathbf{X} = \left[\mathbf{x}(0),...,\mathbf{x}(N-1)\right] \qquad (8)$$

is the vector of the random process at the GR PF output and THR_{GR} is the GR detection threshold.

Under the hypotheses $\mathcal{H}_1$ and $\mathcal{H}_0$ when the amplitude of the transmitted signal is equal to the amplitude of the model signal, $s_i^m[k] = s_i[k]$, $\mu = 1$, the GR decision statistics $T_{GD}(\mathbf{X})$ takes the following form in the statistical sense, respectively:

$$\begin{cases} \mathcal{H}_1 : T_{GD}(\mathbf{X}) = \sum_{k=0}^{N-1}\sum_{i=1}^{M}\{s_i^2[k] + \eta_i^2[k] - \zeta_i^2[k]\} \\ \mathcal{H}_0 : T_{GD}(\mathbf{X}) = \sum_{k=0}^{N-1}\sum_{i=1}^{M}\{\eta_i^2[k] - \zeta_i^2[k]\} \end{cases} . \qquad (9)$$

In (9) the term $\sum_{k=0}^{N-1}\sum_{i=1}^{M}s_i^2[k] = E_s$ corresponds to the average transmitted signal energy, and the term $\sum_{k=0}^{N-1}\sum_{i=1}^{M}\eta_i^2[k] - \sum_{k=0}^{N-1}\sum_{i=1}^{M}\zeta_i^2[k]$ is the background noise at the GR output. The GR output background noise is the difference between the noise power at the GR PF and GR AF outputs. Practical implementation of the GR decision statistics requires an estimation of the noise variance σ_η^2 using the reference noise $\eta_i[k]$ at the AF output.

4 UWB System-Performance Evaluation

The performance of UWB multiuser communication systems based on the generalized approach to signal processing in noise is defined by several factors, including modulation scheme, pulse shape, number of users, and the number of time slots per frame. In this Section, we analyze the *BER* performance for both the pulse position modulation and binary phase-shift keying schemes that utilize the new pulse design.

4.1 Basic Assumptions

Let us first define the assumptions made in our analysis:

1. The *BER* is calculated for a receiver over a single channel carrying signals from multiple wireless users, each randomly transmitting one bit per frame.
2. The system has perfect power control, such that multiuser interference arrives from each wireless unit at the base station receiver with equal power.

Vyacheslav Tuzlukov

3. Synchronization with the desired user is achieved. To simplify calculations, timing jitter and imperfect tracking are not considered.

4. Time of signal arrival for each interferer is modeled as independent uniformly distributed (i.i.d.) random variables over one frame period.

5. User data are binary with the equal probability.

6. User pulse collision is considered without utilizing distinct time-hopping codes for each symbol. In other words, each user has only one hop per symbol, $N_h = 1$.

4.2 *BER* Analysis in Multiuser Environment

Given N_u co-channel users, the received signal from the additive white Gaussian noise (AWGN) channel consists of

$$r(t) = \sum_{k=1}^{N_u} A_k s_k(t - \tau_k) + w(t) \ , \qquad (3)$$

where A_k is the amplitude of the signal received from the k-th transmitter; s_k is the transmitted signal from the k-th transmitter; the random variable τ_k is the time delay between the transmitter k and the receiver, and $w(t)$ is the AWGN. The received signal can be viewed as the desired user's signal plus user interference and noise

$$r(t) = A_1 s_1(t - \tau_1) + \sum_{k=2}^{N_u} A_k s_k(t - \tau_k) + w(t) \ . \quad (4)$$

Without loss of generality, the system performance is characterized by user 1's *BER*. Thus, our subsequent calculations are given for the receiver of user 1.

To begin, the output of the ideal generalized receiver in Fig. 4 is given by

$$y^{(1)}(jT_f) = 2 \int_{jT_f + c_j^{(1)}T_c + \tau_1}^{jT_f + c_j^{(1)}T_c + \tau_1 + T_c} s^m(t - jT_f - c_j^{(1)}T_c - \tau_1) r(t) dt$$

$$- \int_{jT_f + c_j^{(1)}T_c + \tau_1}^{jT_f + c_j^{(1)}T_c + \tau_1 + T_c} r^2(t) dt + \int_{jT_f + c_j^{(1)}T_c + \tau_1}^{jT_f + c_j^{(1)}T_c + \tau_1 + T_c} \eta^2(t) dt \ , \qquad (5)$$

where T_f is the frame duration; T_c is the slot duration; $c_j^{(1)}$ is the j-th bit of the desired transmitter's time-hopping sequence; $\eta(t)$ is the reference noise forming at the GR AF output.
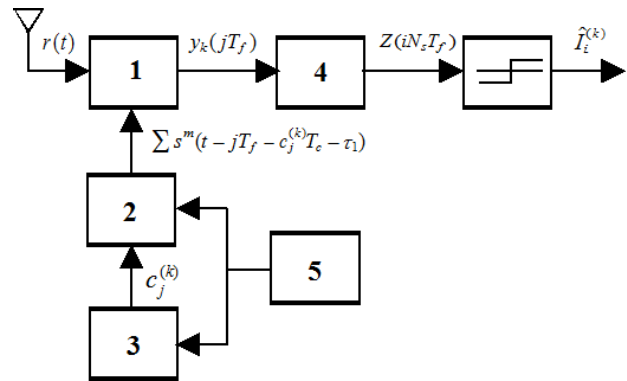
Fig. 4. Block diagram of multiuser generalized receiver
1 – impulse generalized receiver; 2 – generalized receiver mask generator; 3 – time-hopping code generator; 4 – impulse train integrator; 5 – synchronization control.

For the pulse-position modulation (PPM) scheme the correlation mask takes the form

$$s^m(t) = \upsilon_{cor}(t) - \upsilon_{cor}(t - \delta) \ , \qquad (6)$$

while for the binary phase-shifted keying (BPSK) scheme it is simply

$$s^m(t) = \upsilon_{cor}(t) \ . \qquad (7)$$

Note that $\upsilon_{cor}(t)$ is the transmitted pulse shape $s_1^m(t)$, δ is the PPM modulation index.

Substituting (4) into (5), we can write the generalized receiver output in the following form

$$y^{(1)}(jT_f) = \int_{jT_f + c_j^{(1)}T_c + \tau_1}^{jT_f + c_j^{(1)}T_c + \tau_1 + T_c} \left\{ 2s^m(t - jT_f - c_j^{(1)}T_c - \tau_1) \right.$$

$$\times \left| A_1 s_1(t - \tau_1) + \sum_{k=2}^{N_u} A_k s_k(t - \tau_k) + \zeta(t) \right|$$

$$\left. - \left[A_1 s_1(t - \tau_1) + \sum_{k=2}^{N_u} A_k s_k(t - \tau_k) + \zeta(t) \right]^2 + \eta^2(t) \right\} dt$$

$$(8)$$

From (8), a more useful form of $y^{(1)}(jT_f)$ is obtained

$$y^{(1)}(jT_f) = y_s^{(1)}(jT_f) - \sum_{k=2}^{N_u} y_k^{(1)}(jT_f) + y_w^{(1)}(jT_f) \ , (9)$$

where taking into consideration the main functioning condition (4) of the generalized receiver we obtain

$$y_s^{(1)}(jT_f)$$

$$= \int_{jT_f+c_j^{(1)}T_c+\tau_1}^{jT_f+c_j^{(1)}T_c+\tau_1+T_c} 2s^m(t-jT_f-c_j^{(1)}T_c-\tau_1)A_1s_1(t-\tau_1)dt \ ; \tag{10}$$

$$y_k^{(1)}(jT_f) = \int_{jT_f+c_j^{(1)}T_c+\tau_1}^{jT_f+c_j^{(1)}T_c+\tau_1+T_c} \left\{ \left[\sum_{k=2}^{N_u} A_k s_k(t-\tau_k) \right]^2 \right.$$
$$\left. + 2\zeta(t)\sum_{k=2}^{N_u} A_k s_k(t-\tau_k) \right\} dt \ ; \tag{11}$$

$$y_w^{(1)}(jT_f) = \int_{jT_f+c_j^{(1)}T_c+\tau_1}^{jT_f+c_j^{(1)}T_c+\tau_1+T_c} [\eta^2(t)-\zeta^2(t)]dt \ . \tag{12}$$

Here in (9)-(12) the term $y_s^{(1)}(jT_f)$ is the signal component; the term $\sum_{k=2}^{N_u} y_k^{(1)}(jT_f)$ is the interference component; the term $y_w^{(1)}(jT_f)$ is the background noise of the generalized receiver.

If there is only one hop per symbol, $N_h = 1$ then there is no processing gain and the i-th information bit $I_h^{(1)}$ of the user 1 is obtained by sending $y^{(1)}(jT_f)$ through the detector threshold. On the other hand, if the symbol energy is spread over multiple frames, i. e., $N_h > 1$ it is necessary to sum the energy collected from the generalized receiver output over N_h frames, such we obtain

$$\underbrace{\sum_{j=1}^{N_h} y^{(1)}(jT_f)}_{Z(iT_f)} = \underbrace{\sum_{j=1}^{N_h} y_s^{(1)}(jT_f)}_{Z_s(iT_f)}$$
$$+ \underbrace{\underbrace{\sum_{j=1}^{N_h} y_k^{(1)}(jT_f)}_{Z_{in}(iT_f)} + \underbrace{\sum_{j=1}^{N_h} y_w^{(1)}(jT_f)}_{Z_w(iT_f)}}_{Z_{noise}(iT_f)} \ . \tag{13}$$

Upon collecting the energy, $\hat{I}_i^{(1)}$ is determined by the decision rule defined in (14), where $\hat{I}_i^{(1)}$ is the estimate of the i-th information symbol sent by the user 1 $I_i^{(1)}$

$$\hat{I}_i^{(1)} = \begin{cases} 0, & Z(iT_f) > 0 \\ 1, & Z(iT_f) < 0 \end{cases} \ . \tag{14}$$

In this case, the probability of error can be defined in the following way

$$P_{error} = 0.5P(Z_{noise}(iT_f) < -Z_s(iT_f)\,|\,I_i^{(1)}=0)$$

$$+ 0.5P(Z_{noise}(iT_f) < -Z_s(iT_f)\,|\,I_i^{(1)}=1) \ . \tag{15}$$

To calculate the probability of error P_{error} there is a need to define the probability density function of the total noise forming at the receiver output, i.e., $Z_{noise}(iT_f)$ that consists of the summation of N_h independent random variables. The probability density function of $Z_{noise}(iT_f)$ takes the following form

$$f_{Z_{noise}}(z) = \underbrace{f_{Y_{noise}}(y_{noise})*\cdots*f_{Y_{noise}}(y_{noise})}_{N_h \text{ convolutions}} \ , \tag{16}$$

where y_{noise} is the summation of multiuser interference energy plus the background noise forming at the generalized receiver output. The total noise energy is characterized by the McDonald probability density function or approximated Gaussian probability density function [14, Chapter 3, pages 250-263; Chapter 4, pages 324 -328] with the zero mean and variance $4\sigma_w^4$, where σ_w^4 is the variance of the Gaussian noise. However, the multiuser interference $Z_{in}(iT_f)$ is characterized by a distribution determined by $\upsilon_{cor}(t), s^m(t)N_u, N_s, \ T_c$.

To find the probability density function of the interference component $Z_{in}(iT_f)$ it is necessary to first calculate the probability density function for every possible number of collisions. Let p be the probability that a pulse from the user k collides with a pulse of the user 1 and let q be the probability that the user k does not collide with the user 1. A collision occurs when the time of arrival of an undesired user pulse causes interference with the user 1's pulse. As stated in the assumption 4 (see Section 4.1), the probability density function of signal arrival time of the user k is uniform over one frame. Therefore for PPM, the user k's pulse occurs at the time $(jT_f + \tau_k)$ half of the time, and at the time $(jT_f + \tau_k + \delta)$ the other half of the time. Since the modulation of the k-th user is independent of the user 1, user k's PPM can be enveloped into the random variable τ_k without changing its distribution:

$$f_{\tau_k}(\tau_k) = \begin{cases} T_f^{-1}, & 0 \le \tau_k < T_f \\ 0, & otherwise \end{cases} \ . \tag{17}$$

Similarly, for BPSK modulation, the user k's pulse arrives at $(jT_f + \tau_k)$ and the modulation of user k can be ignored, since we define a collision as an undesired pulse interference, either constructive or destructive, with the user 1's pulse.

Vyacheslav Tuzlukov

By modelling the multiuser interference this way, a collision occurs if $\tau_1 - T_m < \tau_k < \tau_1 + T_c$, where T_m is the pulse duration and T_c is the slot duration. Note that p can now be found by integrating the probability density function $f_{\tau_k}(\tau_k)$ over the collision interval as

$$p = \int_{\tau_1 - T_m}^{\tau_1 + T_c} T_f^{-1} d\tau_k = \frac{T_c + T_m}{T_f} = \frac{T_c + T_m}{T_c} \times \frac{1}{N_s} \; ; \quad (18)$$

$$q = 1 - p = 1 - \frac{T_c + T_m}{T_c} \times \frac{1}{N_s} \; , \quad (19)$$

where N_s is the number of slots per frame. Therefore, the probability of having exactly m collisions with the user 1 is defined in the following form

$$p(m) = \binom{N_u - 1}{m} p^m q^{N_u - 1 - m} \; . \quad (20)$$

Note that

$$f_{Y_{noise}}(y_{noise}) = \left[\sum_{m=0}^{N_u - 1} \binom{N_u - 1}{m} p^m q^{N_u - 1 - m} f(y_{noise}|m) \right]$$
$$* f_N(y_k) \quad (21)$$

is the summation of the multiplication of the probability of exactly m collisions with the conditional probability density function $f(y_{noise}|m)$ for all values m convolved with $f_N(y_k)$, where the probability density function $f(y_{noise}|m)$ is the convolution of the probability density function $f_{Y_k}(y_k|1)$ with itself m times and $f_N(y_k)$ is the Gaussian probability density function and

$$f(y_{noise}|m) = \underbrace{f_{Y_k}(y_k|1) * \cdots * f_{Y_k}(y_k|1)}_{m \text{ convolutions}} \; . \quad (22)$$

To find $f_{Y_k}(y_k|1)$, the following random-variable transformation of γ to y_k is used:

$$y_k(\gamma) = \int_0^{T_c} s^m(t) \upsilon_{cor}(t + \gamma) dt \; . \quad (23)$$

The above equation assumes that exactly one collision occurs and that γ is the solution to this equation. Since γ is the uniformly distributed random variable, we can obtain the following conditional probability:

$$f_{Y_k}(y_k|1) = \left[\frac{dy_k(\gamma)}{d\gamma} \right]^{-1} f_\Gamma(\gamma) \; , \quad (24)$$

where

$$f_\Gamma(\gamma) = \begin{cases} \dfrac{1}{T_c + T_m}, & -T_m < \gamma < T_c \\ 0, & otherwise \end{cases} \; . \quad (25)$$

If the closed form for the pulse $\upsilon_{cor}(t)$ is not available, then the transformation of (23) is not possible analytically. However, since γ is the uniformly distributed random variable, the probability density function $f_{Y_k}(y_k|1)$ can be estimated by generating, according to (23), a histogram of $y_k(\gamma)$ from random samples of γ. Once the probability density function $f_{Y_k}(y_k|1)$ is determined, $f(y_{noise}|m)$ can be calculated using (22) before finding $f_{Y_{noise}}(y_{noise})$. Finally, the probability density function of $Z_{noise}(jT_f)$ that allows *BER* analysis, can be calculated using (16).

Since the generalized receiver masks for BPSK and PPM differ, not only in shape, but also in duration, the probability of collision for BPSK is greater than that of PPM. In the ideal case, when there is no channel dispersion, the probability of collision for PPM is $3/(2N_s)$ and for BPSK is $2/N_s$. However, this can be misleading, since the frame time of PPM is twice as large as that of BPSK. If T_f is fixed at the same value for both PPM and BPSK, then twice as many time slots are available for BPSK and the probability of collision is halved, thus becoming $1/N_s$. If the received pulse is time dispersed, then the probability of collision increases from that of the ideal case. It can still be calculated using (17) by modifying T_m to match the width of the extended pulse while leaving T_c unchanged. It is important to realize that the probability of collision increases linearly with the pulse width.

4.3 Analytical *BER* Results

The *BER* is calculated holding T_m constant so that the transmission slot period T_c is fixed according to that modulation scheme is used. Since $T_f = N_s T_c$, the frame period is varied only by N_s. After selecting the pulse shape and modulation scheme, the input parameters of the *BER* calculation are limited to N_u and N_s. The *BER* is calculated for N_s values of 100 and 500 to demonstrate how N_s must be carefully selected, such that system performance is adequate for the expected number of users. Similarly, N_u is varied from 1 to 40, showing performance variations for di-

fferent traffic loads. In our calculations, the pulse was spread over the single frame, $N_h = 1$. Thus, the probability density function $f_{Y_{noise}}(y_{noise})$ is used to determine the probability of error P_{error}.

Our analytical results method followed the form of our derivation utilizing $s_1^m(t)$ as the transmitted pulse shape. Since we do not know a closed form of $s_1^m(t)$, we estimated the probability density function $f_{Y_k}(y_k|1)$ using a histogram of 500 bins on $y_k(\gamma)$ as defined in (23), where the pulse shape $s_1^m(t)$ consisted of 50 000 samples and had the fixed duration T_m of 1 nsec. For BPSK simulations, $s^m(t) = s_1^m(t)$, whereas for PPM modulation, $s^m(t) = s_1^m(t) - s_1^m(t - \delta)$, where the modulation index $\delta = T_m$ was used. For a variety of different scenarios, the *BER* results are given in Figs. 5-8.

The analytical results are intuitively reasonable. As N_u increases, the *BER* degrades, since the probability of collision increases. As N_u increases from a small number of users, the probability of collision increases quickly. However, as N_u becomes large, the rate of increase slows down. This characteristic can be seen in the *BER* curves, as the distance between the curves becomes smaller as the number of users increases. In other words, increasing the number of users in the system has a greater impact on the system with a smaller N_u.

Another observation is on the relationship between the signal-to-noise ratio (*SNR*) and multiuser interference. When the *SNR* is low, the *BER* curves are packed closely together, indicating that the multiuser interference has a little effect. As the *SNR* increases, the impact of the generalized receiver background noise on system performance decreases and the multiuser interference becomes more dominant on system performance. As a result of the multiuser interference, the *BER* reaches a floor determined by the number of users and the number of slots per frame in the system. Since the multiuser interference limits the *BER* performance of UWB communication systems, N_s should be carefully selected to provide an acceptable *BER* performance for the maximum number of users in the system.

It is clear from the results that the increasing slot number N_s can also reduce the probability of collision, which in turn increases the range of *SNR* values unaffected by the multiuser interference. This allows the multiuser *BER* performance to remain close to the single-user *BER* performance for higher *SNR* va-

lues. The number of users N_u has only a small effect on which the *SNR* value the *BER* performance diverges from in the single-user case. Since UWB communication systems must transmit the low-power signals to comply with the standard regulations, these communication systems should be designed under the low *SNR*. Therefore, selecting a large N_s determines the system performance with little effect from N_u.

5 Simulation Conditions and Results

5.1 Simulation Comparisons

To verify the validity of Figs. 5-8, we performed a simulation in which we generated a random message. We used this random message to modulate our pulse shape $s_1^m(t)$, and randomly generated N_u interfering pulses of equal amplitude randomly starting over the frame duration. We then added the desired signal, the overlapping parts of the $N_u - 1$ interfering signals, and the AWGN of the proper variance for the desired *SNR* together and sent the received signal through the generalized receiver. This process was repeated for all combinations of modulation type, number of users, number of slots per frame, and *SNR* values. Figures 9 and 10 demonstrate the measured performance versus the analytical performance using the derivation above. The measured and analytical performances are very similar, with differences resulting from the use of a histogram instead of the actual closed-form solution.

5.2 Multipath Simulation

We also present a simulation result for the UWB communication system under multipath distortions. In this specific example, we make the following assumptions.

- Because of the large frame duration, we assume that the multipath interference received come from the desired user's current bit. Interference from the previous user bits will dissipate well before the next frame starts.
- Our multipath channel is of the form

$$h(t) = \delta(t) + \sum_{i=1}^{L} \beta_i \delta(t - t_i) \quad , \qquad (26)$$

where β_i is the random variable that is normally distributed with the zero mean and variance equal to 0.3; t_i is the random variable uniformly distributed over the interval $[0, kT]$. The value kT is proportional to the time-slot

duration.

- Included in the multipath simulation is also a multiuser simulation with $N_u = 20$, $N_s = 10$. The BPSK modulation was employed.
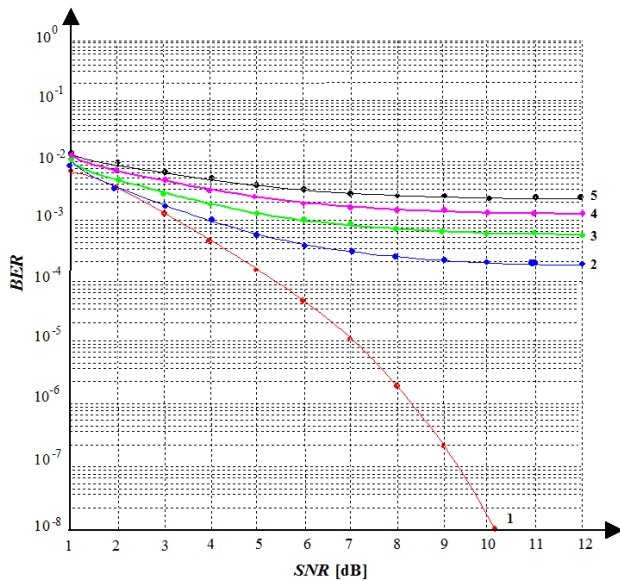
Fig. 5. *BER* for the UWB communications system using BPSK with $N_s = 100$: 1- $N_u = 1$; 2 - $N_u = 10$; 3 - $N_u = 20$; 4 - $N_u = 30$; 5 - $N_u = 40$.
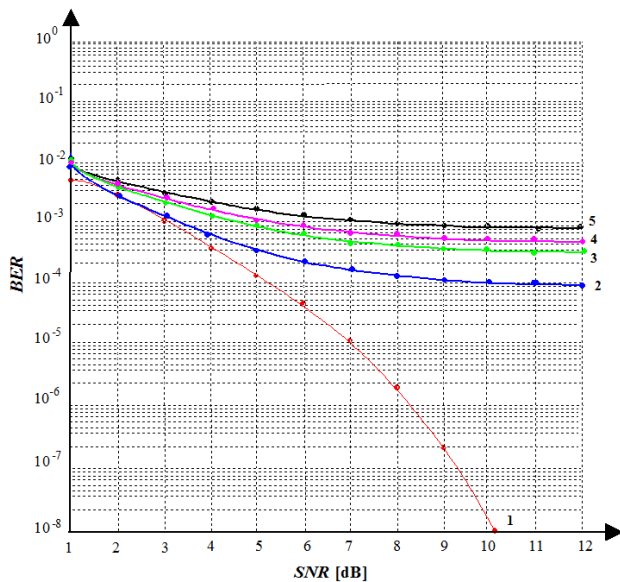
Fig. 6. *BER* for the UWB communications system using BPSK with $N_s = 500$: 1- $N_u = 1$; 2 - $N_u = 10$; 3 - $N_u = 20$; 4 - $N_u = 30$; 5 - $N_u = 40$.

It should be noted that our simulation cases are not general enough for a highly rich scattering environment, since the number of multipaths is low. For each multipath ray, the probability of multipath interference is approximately $1/(kT)$. Thus, if kT is not
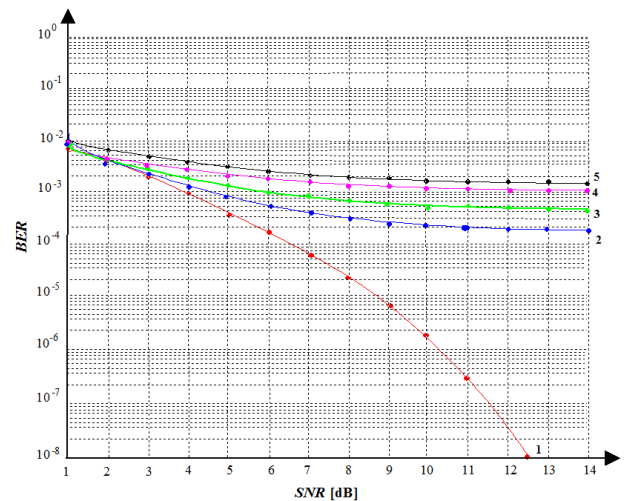
Fig. 7. *BER* for the UWB communications system using PPM with $N_s = 100$: 1- $N_u = 1$; 2 - $N_u = 10$; 3 - $N_u = 20$; 4 - $N_u = 30$; 5 - $N_u = 40$.
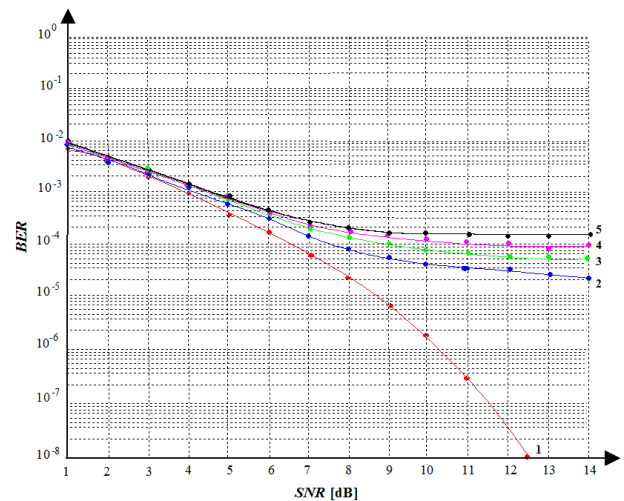
Fig. 8. *BER* for the UWB communications system using PPM with $N_s = 500$: 1- $N_u = 1$; 2 - $N_u = 10$; 3 - $N_u = 20$; 4 - $N_u = 30$; 5 - $N_u = 40$.

small or the number of rays is low, there is a very small effect from the multipath interference. Basically, simulation for multipath is very similar to the multiuser simulation. The difference is that we are confining the arrival of the "users" (rays) to a smaller interval around our desired pulse, thereby increasing our probability of collision. For the 3-ray model, there is no significant multipath interference at $kT > 5$ nsec, and even at $kT = 5$ nsec, since the multipath interference did not cause that large of a shift in the *BER* curves. Increasing the number of rays in Fig. 11 to five and keeping $kT = 5$ nsec, results in a noticeable increase in the *BER* performance. Also, as a random case, we chose 20 rays with $kT = 40$

nsec, and some multipath degradation was noticed in terms of the *BER* performance floor in Fig. 11.
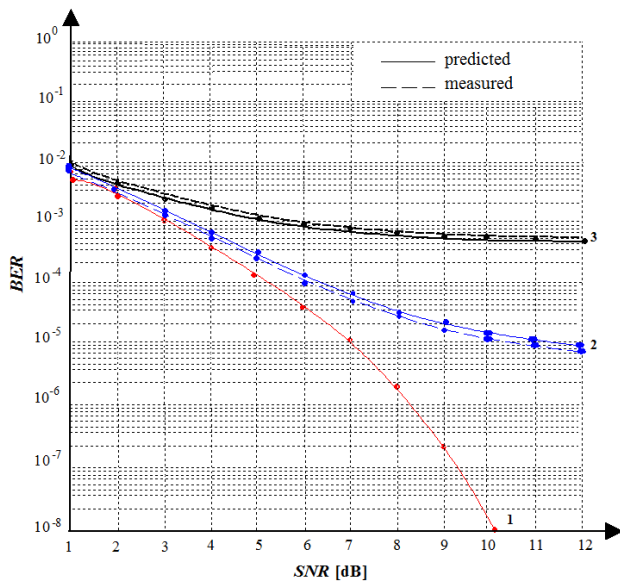
Fig. 9. Comparison of the predicted and measured BPSK performance: 1- $N_u = 1$; 2 - $N_u = 10, N_s = 1000$; 3 - $N_u = 40, N_s = 100$.
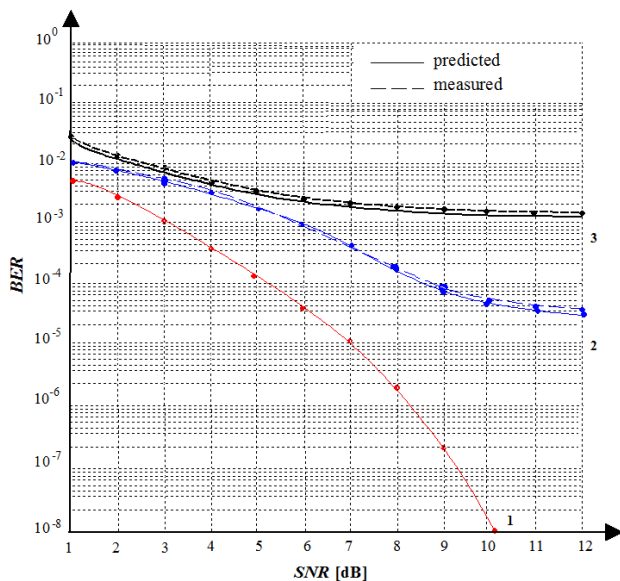
Fig. 10. Comparison of the predicted and measured PPM performance: 1- $N_u = 1$; 2 - $N_u = 10, N_s = 1000$; 3 - $N_u = 40, N_s = 100$.

6 Conclusions

In this paper, we study the system performance of new UWB pulse-shape design algorithm applicable to the UWB communication systems constructed based on the generalized approach to signal processing
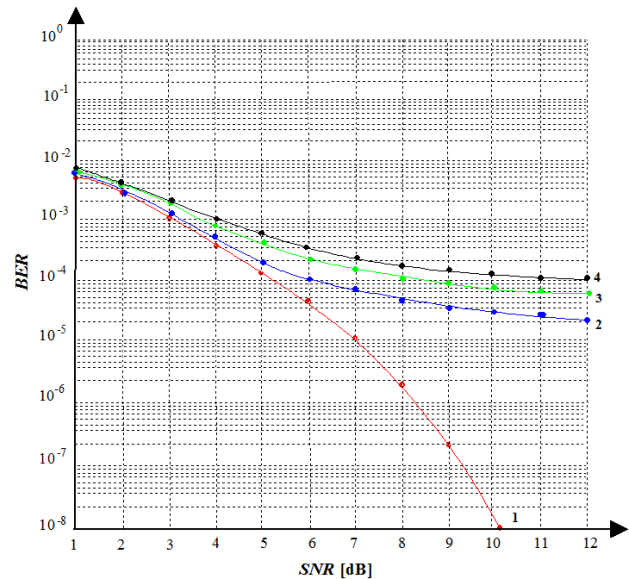
Fig. 11. Effect of multipath for the BPSK system with $N_u = 20$ and $N_s = 100$: 1- $N_u = 1$; 2 – no multipath; 3 – 20 ray $kT = 40$ nsec; 4 – 5 ray $kT = 5$ nsec.

in noise. The theoretical performance of the UWB communication systems constructed based on the generalized approach to signal processing in noise in relation to the selection of the modulation scheme, the number of users, and the number of time slots available per frame is presented. Simulation results are provided as verifications of the analytical approach. In addition, the robustness of the UWB communication systems constructed based on the generalized approach to signal processing in noise against a limited number of multipaths is also demonstrated.

References

[1] J. Forester, E. Green, S. Somayazulu, and D. Leeper, Ultra-wideband technology for short-or medium-range wireless communications//*Intel Technology Journal. Q2*. 2001, Vol. 5, No. 2. pp. 1-11.

[2] M.Z. Win and R.A. Scholtz, Impulse radio: How it works//*IEEE Communications Letters*. 1998, Vol. 2, No. 2, pp. 36-38.

[3] T. Mitchell, Broad is the way//*IEE Review*. 2001, Vol. 47, No. 1. pp. 35-39.

[4] B. Parr, B. Cho, K. Wallace, and Z. Ding, A novel ultra-wideband pulse design algorithm// *IEEE Communications Letter*. 2003, Vol. 7, No. 5, pp. 219-221.

[5] P. Bora, K. Bhattcharyya, Ultra-wide band (UWB) pulse design and channel modeling// *Journal of Telecommunications*. 2018, Vol. 4, No. 2, pp. 1-9

[6]   J. Yan and C. Nguyen, A new ultra-wideband, ultra-short monocycle pulse generator with reduced ringing//*IEEE Microwave Wireless Component Letters.* 2002, Vol. 12, No. 6, pp. 206-208.

[7]   M.H. Hayes, *Statistical Digital Signal Processing and Modeling.* New York: Wiley, 1996.

[8]   B. Li, Z. Zhou, W. Zou, D, Li, C. Zhao, Optimal waveforms design for ultra-wideband impulse radio sensors//*Sensors.* 2010, Vol.10, No.12, pp. 11038-11063.

[9]   A. Valizade, P. Rezaei, A.A. Orouji, A design of UWB reconfigurable pulse transmitter with pulse shape modulation//*Microwave and Optical Technology Letters.* 2016, Vol. 58, No. 9, pp. 2221-2227.

[10] D. Slepian and H.O. Pollak, Prolate spheriodal wave functions, Fourier analysis, and uncertainty-I//*Bell System Technology Journal.* 1961, Vol. 40, No. 1, pp.43-46.

[11] D. Slepian, Prolate spheriodal wave functions, Fourier analysis, and uncertainty-V: The discrete case//*Bell System Technology Journal.* 1978, Vol. 57, No. 5, pp. 1371-1430.

[12] X. Luo, L. Yang, and G.B. Giannakis, Designing optimal pulse-shapers for ultra-wideband radios//*Journal Communication Networks.* 2003, Vol. 5, No. 4, pp. 344-353.

[13] V. Tuzlukov, A new approach to signal detection theory//*Digital Signal Processing: Review Journal.* 1998, Vol.8, No. 3, pp.166–184.

[14] V. Tuzlukov, *Signal Detection Theory.* Springer-Verlag, New York, USA, 2001, 746 pp.

[15] V. Tuzlukov, *Signal Processing Noise.* CRC Press, Boca Raton, London, New York, Washington, D.C., USA, 2002, 692 pp.

[16] M. Maximov, Joint correlation of fluctuative noise at outputs of frequency filters//*Radio Engineering.* 1956, No. 9, pp. 28–38.

[17] Y. Chernyak, Joint correlation of noise voltage at outputs of amplifiers with no overlapping responses//*Radio Physics and Electronics.* 1960, No. 4, pp. 551–561.

[18] Shbat, M., Tuzlukov, V.P. Definition of adaptive detection threshold under employment of the generalized detector in radar sensor systems//*IET Signal Processing.* 2014, Vol. 8, Issue 6, pp. 622–632.

[19] Tuzlukov, V.P. DS-CDMA downlink systems with fading channel employing the generalized//*Digital Signal Processing.* 2011. Vol. 21, No. 6, pp. 725–733.

[20] *Communication Systems: New Research,* Editor: Vyacheslav Tuzlukov, NOVA Science Publishers, Inc., New York, USA, 2013, 423 pp.

[21] Shbat, M., Tuzlukov, V.P. Primary signal detection algorithms for spectrum sensing at low SNR over fading channels in cognitive radio//*Digital Signal Processing* (2019). https://doi.org/10.1016/j.dsp. 2019.07.16. *Digital Signal Processing.* 2019, Vol. 93, No. 5, pp. 187- 207.

[22] V. Tuzlukov, Signal processing by generalized receiver in wireless communications systems over fading channels," Chapter 2 in *Advances in Signal Processing.* IFSA Publishing Corp. Barcelona, Spain. 2021. pp. 55-111.

[23] V. Tuzlukov, Interference Cancellation for MIMO Systems Employing the Generalized Receiver with High Spectral Efficiency//*WSEAS Transactions on Signal Processing.* 2021, Vol. 17, Article #1, pp. 1-15.

[24] M. Shbat and V. Tuzlukov, SNR wall effect alleviation by generalized detector employment in cognitive radio networks//*Sensors,* 2015, 15 (7), pp.16105-16135;doi:10.3390/s150716105.

[25] V. Tuzlukov, Signal processing by generalized detector in DS-CDMA wireless communication systems with frequency-selective channels//*Circuits, Systems, and Signal Processing.* Published on-line on February 2, 2011, doi:10.1007/s00034-011-9273-1; 2011, Vol.30, No.6, pp. 1197–1230.

[26] M. Shbat, V. Tuzlukov, Generalized detector as a spectrum sensor in cognitive radio networks//*Radioengineering.*2015, Vol. 24, No. 2, pp. 558–571.

Dr. Vyacheslav Tuzlukov received the MSc and PhD degrees in radio physics from the Belarusian State University, Minsk, Belarus in 1976 and 1990, respectively, and DSc degree in radio physics from the Kotelnikov Institute of Radioengineering and Electronics of Russian Academy of Sciences in 1995. Starting from 1995 and till 1998 Dr. Tuzlukov was a Visiting Professor at the University of San-Diego, San-Diego, California, USA. In 1998 Dr. Tuzlukov relocated to Adelaide, South Australia, where he served as a Visiting Professor at the University of Adelaide till 2000. From 2000 to 2002 he was a Visiting Professor at the University of Aizu, Aizu-Wakamatsu City, Fukushima, Japan and from 2003 to 2007 served as an Invited Professor at the Ajou University, Suwon, South Korea, within the Department of Electrical and Computer Engineering. Starting from March 2008 to February 2009 he joined as a Full

Professor at the Yeungnam University, Gyeonsang, South Korea within the School of Electronic Engineering, Communication Engineering, and Computer Science. Starting from March 1, 2009 Dr. Tuzlukov served as Full Professor and Director of Signal Processing Lab at the Department of Communication and Information Technologies, School of Electronics Engineering, College of IT Engineering, Kyungpook National University, Daegu, South Korea. Currently, Dr. Tuzlukov is the Head of Department of Technical Exploitation of Aviation and Radio Engineering Equipment, Belarusian State Academy of Aviation, Minsk, Belarus. His research emphasis is on signal processing in radar, wireless communications, wireless sensor networks, remote sensing, sonar, satellite communications, mobile communications, and other signal processing systems. He is the author over 280 journal and conference papers, seventeenth books in signal processing published by Springer-Verlag and CRC Press. Some of them are *Signal Detection Theory* (2001), *Signal Processing Noise* (2002), *Signal and Image Processing in Navigational Systems* (2005)*, Signal Processing in Radar Systems* (2012), Editor of the book *Communication Systems: New Research* (2013), Nova Science Publishers, Inc, USA, and has also contributed Chapters "Underwater Acoustical Signal Processing" and "Satellite Communications Systems: Applications" to *Electrical Engineering Handbook: 3rd Edition*, 2005, CRC Press; "Generalized Approach to Signal Processing in Wireless Communications: The Main Aspects and Some Examples" to *Wireless Communications and Networks: Recent Advances*, InTech, 2012; "Radar Sensor Detectors for Vehicle Safety Systems" to *Electrical and Hybrid Vehicles: Advanced Systems, Automotive Technologies, and Environmental and Social Implications*, Nova Science Publishers, Inc., USA, 2014; "Wireless Communications: Generalized Approach to Signal Processing" and "Radio Resource Management and Femtocell Employment in LTE Networks", to *Communication Systems: New Research*, Nova Science Publishers, Inc., USA, 2013; "Radar Sensor Detectors for Vehicle Safety Systems" to *Autonomous Vehicles: Intelligent Transport Systems and Automotive Technologies*, Publishing House, University of Pitesti, Romania, 2013; "Radar Sensor Detectors for Vehicle Safety Systems," to *Autonomous Vehicles: Intelligent Transport Systems and Smart Technologies*, Nova Science Publishers, Inc., New York, USA, 2014; "Signal Processing by Generalized Receiver in DS-CDMA Wireless Communication Systems," to *Contemporary Issues in Wireless Communications*. INTECH, CROATIA, 2014; "Detection of Spatially Distributed Signals by Generalized Receiver Using Radar Sensor Array in Wireless Communications," to *Advances in Communications and Media Research*. NOVA Science Publishers, Inc., New York, USA, 2015; "Signal Processing by Generalized Receiver in Wireless Communication Systems over Fading Channels" to *Advances in Signal Processing*. IFSA Publishing Corp. Barcelona, Spain.

2021; "Generalized Receiver: Signal Processing in DS-CDMA Wireless Communication Systems over Fading Channels" to *Book Title: Human Assisted Intelligent Computing: Modelling, Simulations and Its Applications*. IOP Publishing, Bristol, United Kingdom, 2022. He participates as the General Chair, Keynote Speaker, Plenary Lecturer, Chair of Sessions, Tutorial Instructor and organizes Special Sections at the major International Conferences and Symposia on signal processing.

Dr. Tuzlukov was highly recommended by U.S. experts of Defence Research and Engineering (DDR& E) of the United States Department of Defence as a recognized expert in the field of humanitarian demining and minefield sensing technologies and had been awarded by Special Prize of the United States Department of Defence in 1999 Dr. Tuzlukov is distinguished as one of the leading achievers from around the world by Marquis Who's Who and his name and biography have been included in the Who's Who in the World, 2006-2013; Who's Who in World, 25th Silver Anniversary Edition, 2008, Marquis Publisher, NJ, USA; Who's Who in Science and Engineering, 2006-2012 and Who's Who in Science and Engineering, 10th Anniversary Edition, 2008-2009, Marquis Publisher, NJ, USA; 2009-2010 Princeton Premier Business Leaders and Professionals Honours Edition, Princeton Premier Publisher, NY, USA; 2009 Strathmore's Who's Who Edition, Strathmore's Who's Who Publisher, NY, USA; 2009 Presidental Who's Who Edition, Presidental Who's Who Publisher, NY, USA; Who's Who among Executives and Professionals, 2010 Edition, Marquis Publisher, NJ, USA; Who's Who in Asia 2012, 2nd Edition, Marquis Publisher, NJ, USA; Top 100 Executives of 2013 Magazine, Super Network Publisher, New York, USA, 2013; 2013/2014 Edition of the Global Professional Network, Business Network Publisher, New York, USA, 2013; 2013/2014 Edition of the Who's Who Network Online, Business Network Publisher, New York, USA, 2014; Online Professional Gateway, 2014 Edition, Business Network Publisher, New York, USA, 2014; 2014 Worldwide Who's Who", Marquis Publisher, NJ, USA; 2015 Strathmore Professional Biographies, Strathmore's Who's Who Publisher, NY, USA; Who's Who in World, 2015, Marquis Publisher, NJ, USA; 2015-2016 Membership in Exclusive Top 100 network of professionals in the world, NY, USA, 2015; 2015 Who's Who of Executives and Professionals Honours Edition, Marquis Publisher, NJ, USA; Worldwide Who's Who – Top 100 Business Networking, San Diego, CA, USA, 2015.

Phone: +37517345328
Email: slava.tuzlukov@mail.ru